

**STUDIES ON POLY(LACTIC ACID) BASED
BLENDS AND TALC REINFORCED COMPOSITES**

SHIKHA JAIN



CENTRE FOR POLYMER SCIENCE AND ENGINEERING

INDIAN INSTITUTE OF TECHNOLOGY, DELHI

MAY 2015

**STUDIES ON POLY(LACTIC ACID) BASED
BLENDS AND TALC REINFORCED COMPOSITES**

by

SHIKHA JAIN

Centre for Polymer Science and Engineering

Submitted

in fulfillment of the requirements of the degree of Doctor of Philosophy

to the



INDIAN INSTITUTE OF TECHNOLOGY, DELHI

MAY 2015

© Indian Institute of Technology Delhi (IITD), New Delhi, 2013

DEDICATED

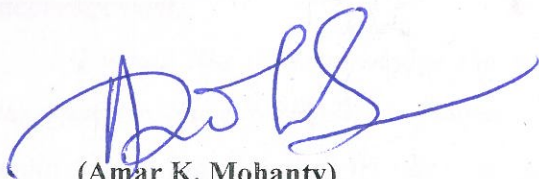
TO MY

PARENTS

CERTIFICATE

This is to certify that the thesis entitled, "Studies on Poly(lactic Acid) based Blends and Talc Reinforced Composites" submitted by Ms. Shikha Jain to the Indian Institute of Technology Delhi, for the fulfillment of award of the degree, Doctor of Philosophy, is a record of bonafide research work carried out by her under our supervision and guidance. This thesis has been prepared in conformity with the rules and regulations of the Indian Institute of Technology Delhi, New Delhi.

The thesis, in our opinion, is worthy of consideration for award of the degree of Doctor of Philosophy in accordance with the regulations of the Institute. To the best of our knowledge, the results embodied in the thesis have not been submitted to any other University or Institute for the award of any other Degree or Diploma.



(Amar K. Mohanty)

Professor

Department of Plant Agriculture & School of
Engineering

University of Guelph,

Ontario, Canada, N1G 2W1



(Anup K. Ghosh)

Professor

Centre for Polymer Science and Engineering

Indian Institute of Technology Delhi

Hauz Khas, New Delhi-110016, India

Acknowledgements

It gives me immense pleasure to express my deep sense of gratitude to all who have helped me along my way through the doctoral studies and a memorable stay at IIT Delhi.

*I express my profound sense of gratitude and veneration to my supervisors, **Prof. Anup K Ghosh** and **Prof. Amar K. Mohanty** for guiding me all the way during my PhD tenure. Their constant inspiration and encouragement have been a great motivation for me behind all the work, I have conducted. I have learnt from them that failures in all doing should motivate one to work harder. They have always boosted me to put in extra efforts and I am indebted to them what I am today. I am also thankful to them for providing me opportunities to handle some short-term projects and assisting them in few industrial projects which enabled me to fortify my skills.*

I would like to thank my research committee members, Prof. Mangla Joshi, Prof. S. N. Maiti and Prof. B. Sathapathy, who have monitored my work and provided me the valuable suggestions. I am also thankful to Prof. V. Choudhary, Prof. A. K. Gupta and Prof. J. Jacob who inspite of their busy schedule have always made themselves available for valuable discussions and support. I would like to convey my special thanks to Prof. Shashi Motilal for her support and encouragement.

I would like to acknowledge the help and support extended by my seniors, Dr. Saikat Banerjee, Dr. Sangita Nandi, Dr. Satpal Singh, Dr. Mayank Dwivedi, for their co-operation. I would like to thank my all friends and colleagues, Priyanka, Sneh, Manash, Tahir, Sanjeev, Jutika, Satish, S. Sabapathy, Priya, Swarna, Savita, Manisha, Khushboo, Bhavna, Naveet, Jaggi, Debang, Dibendu, Astha for their cooperation and friendly attitude. I acknowledge my friend Ms. Megha Singhal for her constant encouragement throughout and immediate help whenever needed.

I would like to extend my thanks to Prof. Manju Misra, University of Guelph, Ontario, Canada for their kind support and providing necessary facilities to carry out research in their laboratory. I would like to thank Dr. Sandeep Ahankari, Dr. Ozgur, Dr. Ranjan Pradhan, Mr. Nima Zaribhakhshs, Dr. Murali M. Reddy, Dr. Sanjeev, Dr. Vivek, Mr. Malaya Nanda, Mr.

Ryan, Ms. Saswata Sahoo, Ms. Binu Kalita, Ms. Sara Bonham, for their co-operation and friendly attitude during my research at University of Guelph, Ontario, Canada.

I owe thanks to laboratory staffs Mr. Surender Sharma, Mr. Ashok Kapoor, Mr. Shiv Kant, Mr. S. S. Bhatnagar for their timely help and suggestions. I would also like to convey my thanks to Ms. Rama Sharma, Suchitra Singh, Mamata, Shalini and Mr. Narender Kumar for their all possible supports. I am grateful to Mr. D. C. Sharma and Mr. Kuldeep of SEM facility (central) for teaching and allowing me to do scan of my samples using the SEM instrument.

I wish to acknowledge Council of Scientific & Industrial Research (CSIR), New Delhi, India for providing me financial assistance (Senior Research Fellowship) to carry out my research work smoothly. I would also like to acknowledge the Department of Foreign Affairs and International Trade (DFAIT), Canada, and the Canadian Bureau for International Education (CBIE) for providing a Graduate Student Exchange Program (GSEP) 2009–2010 fellowship.

I take this opportunity to express my deepest gratitude to my family members. The love from my parents has always given me the strength and confidence to overcome the difficulties and to accomplish the objectives in my life. They always stood by my side with their emotional support, wordly wisdom and blessings. My husband, sisters and brother have always supported me with their unconditional love and care and my deep regards are always with them who have been with me.

Finally and above all, I would like to thank the Almighty God. It would not have been possible for me to reach at this stage of academic pursuit without his grace.

Date

Shikha Jain

Place: New Delhi

Abstract

Increasing environmental concern and limited resources of petroleum has necessitated the use of biodegradable plastics for various applications. Polymers poly(lactic acid) (PLA) is renewable resource based polyester with superior mechanical properties (tensile strength, modulus), optical properties (gloss, transparency) and biodegradability. PLA is associated with some challenges such as low elongation, low impact strength, slow crystallization rate and low melt strength. Elongation of PLA can be increased by blending of PLA with another flexible biodegradable polymer. Polycaprolactone (PCL) is a synthetic biodegradable polymer having high elongation and toughness and flexibility. Blending of PCL into PLA is a promising approach to increase elongation and toughness of PLA. Extent and rate of crystallization can enhance by adding nucleating agent in to PLA. Talc works as nucleating agent as well as reinforcing filler and increase thermal and mechanical properties and crystallinity of polymer matrix.

The objective of the present study was to study the effect of PCL and talc on structure, processability and properties of PLA and to investigate thermal, morphological, mechanical, rheological and barrier properties in detail. In the present work, PLA/talc composites, PLA/PCL blends and PLA/PCL/talc composites were developed by melt-mixing in twin screw extruder followed by blown film processing and injection molding. Developed PLA based blends and composites were analyzed by using various characterization techniques including thermal, rheological, morphological, barrier, tensile, biodegradability etc.

Isothermal and nonisothermal crystallization kinetics of PLA was studied in presence of talc at different crystallization temperatures and different cooling rates and analyzed by using Avrami equation. Talc worked as nucleating agent and increased degree of crystallinity 30% in neat PLA to 35% in PLA/talc composites. Talc has accelerated the crystallization of PLA and significantly

reduced crystallization half time ($t_{1/2}$) where it was 9.5 min in neat PLA and 1.1 min in PLA/talc-5 composites at 120 °C. Activation energy barrier (ΔE_a) of crystallization was also reduced significantly in presence of talc and ΔE_a for neat PLA was -0.8 KJ/mol and -23.2 KJ/mol for PLA/talc-5 composite. Spherulite morphology of PLA/talc composites showed that talc filled system has increased nucleation density and reduced spherulite radius compared to that of neat PLA. Morphology of PLA/talc composites showed random dispersion of talc particles in PLA matrix. Tensile properties evaluation results that talc reinforced composites has increased modulus compared to neat PLA. Water vapor permeability and biodegradability of PLA did not change significantly in presence of talc. PLA/PCL blend showed typical domain-bulk phase morphology where minor phase PCL was dispersed as discrete domains in continuous phase of PLA matrix. PCL blends have increased elongation and toughness with a decrease in tensile modulus and strength. Strain at break in neat PLA was 13% and increased upto 322% in PLA/PCL blend whereas PCL content was 60 wt% in the blend. PLA/PCL blend has increased degree of crystallinity, increased water vapor barrier properties and increased biodegradability compared to neat PLA films.

TABLE OF CONTENTS

	Page number
Certificate	i
Acknowledgement	ii
Abstract	iv
List of Figures	xiii
List of Tables	xx
Abbreviation used	xxii

Chapter 1- Introduction and Literature Survey

1.1 Introduction.....	1
1.2 Biopolymers.....	4
1.2.1 Synthetic biopolymers	5
1.2.2 Natural biobased polymers	7
1.3 Introduction of Poly(lactic acid) (PLA).....	8
1.3.1 Production of PLA	9
1.4 Structure and properties of PLA	10
1.4.1 Crystal Structure of PLA	11
1.4.2 Thermal and crystallization behavior of PLA.....	11
1.4.3 Rheological behavior of PLA	13
1.4.4 Processing of PLA	14
1.4.4.1 Film processing of PLA	14
1.4.5 Physical and mechanical characteristics of PLA	16
1.5 Application and commercial production of PLA.....	17
1.6 PLA based blends	20
1.6.1 PLA/non-biodegradable polymer blends	21
1.6.2 PLA/biodegradable polymer blends	22
1.6.2.1 PLA/PCL blends	25
1.7 PLA based composites.....	26
1.7.1 PLA/natural fiber reinforced composite	27

1.7.2 PLA/synthetic fiber reinforced composites	28
1.7.3 PLA/organic filler reinforced composites.....	28
1.7.4 PLA/inorganic filler composites	29
1.7.4.1 PLA/talc composites	30
1.8 Scope, objectives and plan of work	32
1.8.1 Scope of the work	32
1.8.2 Objectives and plan of work	33
1.9 Format of Thesis	34

Chapter 2- Materials and Experimental Methods

2.1 Introduction.....	37
2.2 Raw materials.....	37
2.2.1 Poly(lactic acid) (PLA)	37
2.2.2 Poly(caprolactone) (PCL)	38
2.2.3 Talc	38
2.3 Processing of PLA based blends and composites	39
2.3.1 Processing in twin screw extruder	39
2.3.2 Micro injection molding	42
2.3.3 Blown film processing	42
2.4 Characterization techniques	43
2.4.1 Scanning electron microscopic analysis of PLA based blends and composites	44
2.4.2 Polarized light optical microscopic analysis of PLA based blends and composites.....	44
2.4.3 Differential scanning calorimetric (DSC) analysis of PLA based blends and composites.....	46
2.4.3.1. Crystallization kinetics of neat PLA and PLA/talc composites.....	47
2.4.4 Thermogravimetric analysis (TGA) of PLA based blends and composites	47
2.4.5 Dynamic mechanical analysis (DMA) of PLA based blends and composites.....	48
2.4.6 Rheological study of PLA based blends and composites by capillary rheometry.....	49
2.4.7 Rheological study of PLA based blends and composites by parallel plate rheometer	50
2.4.8 Melt flow index (MFI) measurement of PLA based blends and composites	51

2.4.9 Tensile testing of PLA based blends and composites	51
2.4.10 Wide angle X-ray diffraction (WAXD) study of PLA based blends and composites blown film.....	52
2.4.11 Water vapor transmission rate (WVTR) measurement of PLA based blends and composites.....	53
2.4.12 Compostability of PLA based blends and composites blown films	53

Chapter 3 - Morphological Behavior of PLA based Blends and Composites

3.1. Introduction.....	55
3.1.1. Spherulite morphology.....	55
3.1.2. Morphology of polymer blends	57
3.1.3. PLA/PCL blends	59
3.2. Experimental	60
3.3. \esults and discussion.....	60
<i>Section 3 A: PLA/talc Composites</i>	<i>61</i>
3A.1 Bulk phase morphology of PLA/talc composites	61
3A.2 Tensile properties of PLA/talc composites	62
3A.2.1 Theoretical prediction of tensile modulus of PLA/talc composites.....	64
3A.3 Spherulite morphology of PLA/talc composites	66
3A.3.1 Spherulite morphology after etching of amorphous phase of spherulite.....	68
3A.4 Effect of different crystallization temperatures on spherulite morphology	70
3A.5 Effect of different cooling rates on spherulite structure	72
<i>Section 3B: PLA/PCL Blends.....</i>	<i>75</i>
3B.1 Bulk phase morphology of PLA/PCL blends.....	75
3B.2 Tensile properties of injection molded PLA/PCL blends specimens.....	79
3B.3 Spherulite morphology of PLA/PCL blends	83
3B.3.1 Spherulite growth rate in PLA/PCL blends.....	85
3B.3.2 Spherulite morphology after etching of amorphous phase.....	86
<i>Section 3C: PLA/PCL/talc Composites</i>	<i>89</i>
3C.1 Bulk phase morphology of PLA/PCL/talc composites	89
3C.2 Tensile properties of PLA/PCL/talc composites	90

3C.3 Spherulite morphology of PLA/PCL/talc composite	94
3.4.	
Conclusions.....	95

Chapter 4 - Thermal Behavior of PLA based Blends and Composites

4.1. Introduction.....	97
4.1.1. Polymer crystallization process: an overview.....	97
4.1.2. Isothermal and non-isothermal crystallization kinetics	99
4.2. Experimental	101
4.3. Results and Discussion	101
<i>Section 4 A: PLA/talc Composites</i>	102
4A.1 Thermal behavior of PLA by DSC	102
4A.2 Isothermal crystallization kinetics of PLA/talc composites.....	104
4A.2.1 Relative crystallinity of isothermal crystallization of PLA/talc composites.....	105
4A.2.2 Avrami exponent and nucleation behavior of PLA/talc composites.....	107
4A.2.3 Crystallization half time ($t_{1/2}$) of PLA/talc composites.....	109
4A.2.4 Activation energy (ΔE_a) of isothermal crystallization of PLA/talc composites ..	111
4A.3 Nonisothermal crystallization kinetics of PLA/talc composites	112
4A.3.1 Thermal behavior of PLA at different cooling rates by DSC	112
4A.3.2 Heat flow curves of nonisothermal crystallization of PLA/talc composites.....	114
4A.3.3 Relative Crystallinity of nonisothermal crystallization of PLA/talc composites.	116
4A.3.4 Avrami exponent and nucleation behavior in nonisothermal crystallization.....	118
4A.3.5 Activation energy barrier of nonisothermal crystallization	120
4A.4 Thermogravimetric analysis (TGA) of PLA/talc composites	121
<i>Section 4B: PLA/PCL Blends</i>	123
4B.1 Thermal behavior of PLA/PCL blends by DSC.....	123
4B.2 Thermogravimetric analysis (TGA) of PLA/PCL blends	126
<i>Section 4C: PLA/PCL/Talc Composites</i>	129

4C.1 Thermal behavior of PLA/PCL/talc composites by DSC	129
4C.2 Thermogravimetric analysis (TGA) of PLA/PCL/talc composites by DSC	131
4.4. Conclusions.....	132

Chapter 5 - Rheological Behavior and Blown Film Characteristics of PLA based Blend and Composite Films

5.1 Introduction.....	134
5.1.1. Blown film processing	134
5.1.2. Dynamic (oscillatory) rheology	135
5.2 Experimental	137
5.3 Results and discussion	137
<i>Section 5A: PLA/talc Composites</i>	138
5A.1 Capillary rheometry of PLA/talc composites.....	138
5A.2 Blown film processing of PLA/talc composites	140
5A.3 Oscillatory shear rheology (parallel plate rheometry) of PLA/talc composites.....	144
5A.3.1 Amplitude sweep of PLA/talc composites.....	144
5A.3.2 Frequency sweep of PLA/talc composites.....	145
<i>Section 5B: PLA/PCL Blends</i>	147
5B.1 Capillary rheometry of PLA/PCL blend	147
5B.2 Blown film processing of PLA/PCL blend	149
5B.3 Oscillatory shear rheology of PLA/PCL blend	152
5B.3.1 Amplitude sweep of PLA and PCL.....	152
5B.3.2 Frequency sweep of PLA/PCL blends	153
<i>Section 5C: PLA/PCL/talc Composites</i>	156
5C.1 Capillary rheometry of PLA/PCL/talc composites	156
5C.2 Blown film processing of PLA/PCL/talc composites	158
5C.3 Oscillatory shear rheology of PLA/PCL/talc composites	160
5.4 Conclusions.....	163

Chapter 6 - Tensile, Barrier Properties and Biodegradability of PLA based Blend and Composite Blown Films

6.1 Introduction.....	165
6.2 Experimental.....	167
6.3 Results and Discussion	167
<i>Section 6A: PLA/talc Composite Blown Films</i>	<i>168</i>
6A.1 Tensile properties of PLA/talc composite blown films	168
6A.2 Dynamic mechanical analysis (DMA) of PLA/talc composites	169
6A.3 Water vapor permeability (WVP) of PLA/talc composite blown films.....	171
6A.3 FTIR analysis of PLA/talc composite blown films.....	172
6A.4 X-ray diffraction (XRD) analysis of PLA/talc composite blown film.....	173
6A.5 Compostability of PLA/talc composite blown films.....	175
<i>Section 6B: PLA/PCL Blend Blown Films.....</i>	<i>178</i>
6B.1 Tensile properties of PLA/PCL blend blown film	180
6B.2 Water vapor permeability (WVP) of PLA/PCL blend blown films.....	181
6B.3 FTIR analysis of PLA/PCL blend blown films.....	182
6B.4 X-ray diffraction (XRD) analysis of PLA/PCL blown film.....	184
6B.5 Compostability of PLA/PCL blend films of PLA/PCL blend blown films	188
<i>Section 6C: PLA/PCL/talc Composite Blown Films.....</i>	<i>188</i>
6C.1 Tensile properties of PLA/PCL/talc composite blown films	189
6C.2 X-ray diffraction (XRD) analysis of PLA/PCL/talc composite blown films.....	198
6.4 Conclusions.....	190

Chapter 7 - Summary and Conclusions

7.1 Background.....	192
7.2 Summary.....	192
7.2.1 Morphological behavior of PLA based blends and composites.....	192
7.2.1.1 PLA/talc composites.....	192
7.2.1.2 PLA/PCL blends.....	193

7.2.1.3 PLA/PCL/talc composites.....	194
7.2.2 Thermal behavior of PLA based blends and composites.....	194
7.2.2.1 PLA/talc composites.....	194
7.2.2.2 PLA/PCL blends.....	195
7.2.2.3 PLA/PCL/talc composites.....	196
7.2.3 Rheological behavior and blown film characteristics of PLA based blends and composites.....	196
7.2.3.1 PLA/talc composites.....	196
7.2.3.2 PLA/PCL blends.....	196
7.2.3.3 PLA/PCL/talc composites.....	197
7.2.4 Tensile, barrier properties and biodegradability of PLA based blend and composite blown films.....	197
7.2.3.1 PLA/talc composites.....	197
7.2.3.2 PLA/PCL blends.....	198
7.2.3.3 PLA/PCL/talc composites.....	198
7.3 Conclusions.....	198
7.4 Scope of future work.....	199
References	211

List of Publication and Biography

LIST OF FIGURES

Sr. No.	Title
Chapter 1	
Figure 1.1	Structure-properties-processing correlations in polymer
Figure 1.2	Schematic presenting advantages and challenges in PLA
Figure 1.3	Life cycle of poly(lactic acid) (PLA)
Figure 1.4	Classification of biopolymers
Figure 1.5	(a) Synthesis of PLA from different route (b) three diastereomeric structures of lactide
Figure 1.6	Stereochemical structure of (a) poly(L-lactide), (b) poly(D-lactide), (c) poly(D,L-lactide)
Figure 1.7	Reinforcement for PLA based composites
Figure 1.8	Chemical structure of talc ($\text{Mg}_3\text{Si}_4\text{O}_{10}(\text{OH})_2$)
Figure 1.9	Schematic work plan for processing and characterization of PLA based blends and composites
Chapter 2	
Figure 2.1	Co-rotating twin screw extruder (Thermo Fisher)
Figure 2.2	Screw profile for the twin screw extruder
Figure 2.3	Haake Minijet microinjection molding
Figure 2.4	Schematic of blown film processing
Figure 2.5	Scanning electron microscope (Carl Zeiss EVO50)
Figure 2.6	Polarized optical light microscope (Meiji Techno) equipped with Instech hot stage
Figure 2.7	DSCQ-200 differential scanning calorimeter (TA instruments, USA)
Figure 2.8	Pyris6 thermo gravimetric analyzer (Perkin Elmer Inc., USA)
Figure 2.9	DMA-Q800 dynamic mechanical analyzer (TA Instrument, USA)
Figure 2.10	Rosand RH7 capillary rheometer (Malvern)
Figure 2.11	Parallel plate rheometer MCR52 (Anton Paar)
Figure 2.12	Dynisco melt flow indexer

- Figure 2.13 Universal testing machine (Zwick Z010)
- Figure 2.14 X-ray diffractometer (X'Pert PRO)
- Figure 2.15 Water vapor permeability tester (Lyssy OPT-5000)

Chapter 3

- Figure 3.1 Spherulite formation from radially grown lamellae
- Figure 3.2 SEM images of cryofractured surface of (a) PLA, (b) PLA/talc-1, (c) PLA/talc-3, (d) PLA/talc-5, (e) talc
- Figure 3.3 Tensile properties of PLA/talc composites injection molded specimens
- Figure 3.4 SEM images of tensile fractured surface of (a) PLA, (b) PLA/talc-1 (c) PLA/talc-3, (d) PLA/talc-5 composites
- Figure 3.5 Theoretical prediction of tensile modulus of PLA/talc composites
- Figure 3.6 Spherulite morphology of (a) PLA (b) PLA/talc-1, (c) PLA/talc-3, (d) PLA/talc-5 composites (obtained from POLM, at 140 °C)
- Figure 3.7 SEM images of PLA spherulites after etching of amorphous phase at different concentration of NaOH (a) 1.0 gm/mol, (b) 0.025 gm/mol
- Figure 3.8 SEM images of crystallized samples of (a) PLA, (b) PLA/talc-1, (c) PLA/talc-3, (d) PLA/talc-5 composites after etching of amorphous phase
- Figure 3.9 SEM images of neat PLA spherulites at different crystallization temperatures
- Figure 3.10 SEM images of PLA/talc-3 composite at different crystallization temperatures
- Figure 3.11 SEM images of neat PLA crystallized at different cooling rates (a) 2 °C/min, (b) 5 °C/min, (c) 10 °C/min, (d) 15 °C/min, (e) 20 °C/min
- Figure 3.12 SEM images of PLA/talc-3 composite crystallized at different cooling rates (a) 2 °C/min, (b) 5 °C/min, (c) 10 °C/min, (d) 15 °C/min, (e) 20 °C/min
- Figure 3.13 Morphology of (a) PLA, (b) PLCL-90/10 (c) PLCL-80/20, (d) PLCL-70/30, (e) PLCL-60/40, (f) PLCL-50/50, (g) PLCL-40/60, (h) PCL (before etching of PCL phase)
- Figure 3.14 Morphology of (a) PLA (b) PLCL-90/10 (c) PLCL-80/20, (d) PLCL-70/30, (e) PLCL-60/40, (f) PLCL-50/50, (g) PLCL-40/60, (h) PCL (after etching of PCL phase)

- Figure 3.15 Domain size and distribution of PCL phase in PLA/PCL blend: (a) PLCL-90/10, (b) PLCL-80/20, (c) PLCL-70/30, (d) PLCL-60/40, (e) PLCL-50/50
- Figure 3.16 PCL domain size in PLA/PCL blends
- Figure 3.17 (a) Tensile modulus (b) tensile stress (c) elongation (d) toughness (e) injection molded specimens of PLA/PCL blends
- Figure 3.18 Stress-strain curves of PLA/PCL blends
- Figure 3.19 SEM images of tensile fractured surface of (a) PLA, (b) PLCL-90/10, (c) PLCL-80/20 (d) PLCL-70/30, (e) PLCL-60/40, (f) PLCL-50/50, (g) PLCL-40/60 (mag. 5KX)
- Figure 3.20 Spherulite morphology of (a) PLA, (b) PLCL-90/10, (c) PLCL-80/20, (d) PLCL-70/30, (e) PLCL-60/40, (f) PLCL-50/50, (from POLM, at 140 °C)
- Figure 3.21 Spherulite radius as a function of time for PLA/PCL blends
- Figure 3.22 SEM images of spherulites in (a) PLA, (b) PLCL-90/10, (c) PLCL-80/20, (d) PLCL-70/30, (e) PLCL-60/40, (f) PLCL-50/50 (after etching of amorphous phase, mag. 1.5KX)
- Figure 3.23 SEM images of spherulites of (a) PLCL-90/10, (b) PLCL-80/20, (c) PLCL-70/30, (d) PLCL-50/50, (e) and (f) PLCL-40/60 (after etching of amorphous phase, mag. 2.5KX)
- Figure 3.24 Morphology of PLA/PCL/talc composites before etching of PCL phase, (a) PLCL-60/40, (b) PLCL-6040-T1, (c) PLCL-60/40-T3, (d) PLCL-60/40-T5 (mag. 5KX)
- Figure 3.25 Morphology of PLA/PCL/talc composites after etching of PCL phase (a) PLCL-60/40, (b) PLCL-6040-T1, (c) PLCL-60/40-T3, (d) PLCL-60/40-T5, (mag. 5KX)
- Figure 3.26 Tensile properties of PLA/PCL/talc composites (a) tensile modulus (b) tensile stress at yield (c) % strain at break (d) toughness (e) stress strain curve
- Figure 3.27 SEM images of tensile fractured surface of (a) PLA (b) PLCL-60/40 (c) PLCL-60/40-T1 (d) PLCL-60/40-T3 (e) PLCL-60/40-T5
- Figure 3.28 Spherulite Morphology of PLA/PCL/talc composites after amorphous phase etching (a) PLCL-60/40 (b) PLCL-6040-T1 (c) PLCL-60/40-T3 (d) PLCL-60/40-T5 (mag. 5KX)

Chapter 4

- Figure 4.1 Melting endotherm of PLA/talc composites from DSC scan
- Figure 4.2 Cooling exotherm of PLA/talc composites from DSC scan
- Figure 4.3 Heat flow curves at different crystallization temperature for (a) PLA, (b) PLA/talc-1, (c) PLA/talc-3, (d) PLA/talc-5 composites
- Figure 4.4 Relative crystallinity at different crystallization temperature for (a) PLA, (b) PLA/talc-1, (c) PLA/talc-3, (d) PLA/talc-5 composites
- Figure 4.5 Avrami plots of $\ln[-\ln(1-\alpha)]$ versus $\log(t)$ at different crystallization temperature for (a) PLA, (b) PLA/talc-1, (c) PLA/talc-3, (d) PLA/talc-5 composites
- Figure 4.6 Crystallization half time ($t_{1/2}$) as a function of crystallization temperature for PLA/talc composites
- Figure 4.7 Plot of $(1/n)\ln(k)$ versus $1/T_c$ for PLA/talc composites for determination of activation energy
- Figure 4.8 Cooling exotherms of neat PLA at different cooling rates from DSC scan
- Figure 4.9 Melting endotherms of neat PLA at different heating rates from DSC scan
- Figure 4.10 Heat flow curves at different cooling rates for (a) PLA, (b) PLA/talc-1, (c) PLA/talc-3, (d) PLA/talc-5 composites
- Figure 4.11 Relative crystallinity as a function of crystallization temperature at different cooling rates for (a) PLA, (b) PLA/talc-1, (c) PLA/talc-3, (d) PLA/talc-5 composites
- Figure 4.12 Relative crystallinity as a function of crystallization time at different cooling rates for (a) PLA, (b) PLA/talc-1, (c) PLA/talc-3, (d) PLA/talc-5 composites
- Figure 4.13 Avrami plots of $\log[-\ln(1-\alpha)]$ versus $\log(t)$ during nonisothermal crystallization kinetics for (a) PLA, (b) PLA/talc-1, (c) PLA/talc-3, (d) PLA/talc-5 composites
- Figure 4.14 Activation energy of crystallization for PLA/talc composites by (a) Kissinger method, (b) Augis-Bennet method
- Figure 4.15 Weight loss curves of PLA/talc composites from TGA
- Figure 4.16 Derivative weight loss curves (DTGA) of PLA/talc composites from TGA
- Figure 4.17 Melting endotherm of PLA/PCL blends from DSC scan
- Figure 4.18 Cooling exotherm of PLA/PCL blends from DSC scan
- Figure 4.19 Weight loss curves of PLA/PCL blends from TGA

- Figure 4.20 Derivative weight loss (DTGA) curves of PLA/PCL blends from TGA
- Figure 4.21 Melting endotherm of PLA/PCL/talc composites from DSC scan
- Figure 4.22 Cooling exotherm of PLA/PCL/talc composites from DSC scan
- Figure 4.23 Weight loss curves of PLA/PCL/talc composites from TGA

Chapter 5

- Figure 5.1 Schematic of stress response to oscillatory strain deformation for an (a) elastic solid (b) viscous fluid (c) viscoelastic material
- Figure 5.2 Shear viscosity as a function of shear rate for PLA/talc composites
- Figure 5.3 Extensional viscosity as a function of extensional rate for PLA/talc composites
- Figure 5.4 (a) Stable bubble of PLA, (b) blown film of PLA, (c) blown film of PLA/talc-3 composite
- Figure 5.5 Draw down ratio (DDR) as a function of nip roll speed for PLA and PLA/talc-3 composite
- Figure 5.6 Storage modulus as a function of amplitude (% strain) for PLA and PLA/talc-3 composite
- Figure 5.7 Loss modulus as a function of amplitude (% strain) % strain for PLA and PLA/talc-3 composite
- Figure 5.8 Storage modulus (G') as a function of frequency for PLA/talc composites
- Figure 5.9 Loss modulus (G'') as a function of frequency for PLA/talc composites
- Figure 5.10 Complex viscosity (η^*) as a function of frequency for PLA/talc composites
- Figure 5.11 Damping ($\tan \delta$) as function of frequency for PLA/talc composites
- Figure 5.12 Shear viscosity as a function of shear rate for PLA/PCL blends
- Figure 5.13 Extensional viscosity as a function of extensional rate for PLA/PCL blends
- Figure 5.14 Blown films of (a) PLA, (b) PLCL-90/10, (c) PLCL-80/20, (d) PLCL-70/30, (e) PLCL-60/40, (f) PLCL-50/50 blends
- Figure 5.15 Morphology development and stretching of dispersed domains in immiscible polymer blends during blown film processing
- Figure 5.16 Morphology of PLA/PCL blend blown films after etching of PCL phase
- Figure 5.17 Amplitude sweep curves (a) storage modulus (b) loss modulus for PLA and PCL for determination of linear viscoelastic region (LVR)

- Figure 5.18 Storage modulus (G') as a function of frequency for PLA/PCL blends
- Figure 5.19 Loss modulus (G'') as a function of frequency for PLA/PCL blends
- Figure 5.20 Complex viscosity (η^*) as a function of frequency for PLA/PCL blends
- Figure 5.21 Cole-Cole plots for PLA/PCL blends
- Figure 5.22 Shear viscosity as a function of shear rate for PLA/PCL/talc composites
- Figure 5.23 Extensional viscosity as a function of extensional rate for PLA/PCL/talc composites
- Figure 5.24 Blown films of (a) PLA/PCL blend and (b) PLCL-60/40-T3 composite
- Figure 5.25 Storage modulus (G') as a function of frequency for PLA/PCL/talc composites
- Figure 5.26 Loss modulus (G'') as a function of frequency for PLA/PCL/talc composites
- Figure 5.27 Damping ($\tan \delta$) as a function of frequency for PLA/PCL/talc composites
- Figure 5.28 Complex viscosity (η^*) as a function of frequency for PLA/PCL/talc composites
- Figure 5.29 Cole-Cole plot for PLA/PCL/talc composites

Chapter 6

- Figure 6.1 Tensile properties (a) tensile modulus (b) tensile stress (c) % strain at break (d) stress-strain curves for PLA and PLA/talc composite blown films
- Figure 6.2 Dynamic mechanical properties (a) storage modulus (b) loss modulus (c) $\tan \delta$ as a function of temperature for PLA/talc composites
- Figure 6.3 FTIR spectrum for PLA and PLA/talc composites
- Figure 6.4 X-ray diffraction pattern for PLA and PLA/talc composites
- Figure 6.5 Percentage weight loss in PLA and PLA/talc composite films as a function of buried time in compost
- Figure 6.6 Blown film samples of (a) PLA and (b) PLA/talc-5 composite film recovered at different from compost
- Figure 6.7 Surface morphology of (a) PLA (b) PLA/talc-5 composite blown films after composting at different time
- Figure 6.8 Tensile properties (a) modulus (b) stress (c) % strain at beak for PLA/PCL blends blown films
- Figure 6.9 Stress strain curves for PLA/PCL blend films during tensile testing
- Figure 6.10 water vapor permeability as a function of PCL wt% in PLA/PCL blends

- Figure 6.11 (a) FTIR spectrum for PLA/PCL blend blown films (b) carbonyl peak enlarge
- Figure 6.12 (a) X-ray diffraction analysis for PLA/PCL blend blown films (b) area under the curve (c) % crystallinity of PLA/PCL blown films from XRD
- Figure 6.13 Percentage weight loss in PLA/PCL blend films as a function of sample buried time in compost
- Figure 6.14 Percentage weight loss in PCL films as a function of sample buried time in compost
- Figure 6.15 Surface morphology of (a) PLA (b) PLCL-80/20, (c) PLCL-60/40, (d) PLCL-40/60, (e) PCL blown films after composting at different time
- Figure 6.16 Tensile properties (a) tensile modulus (b) tensile stress (c) % strain at break (d) stress-strain curves for PLA/PCL/talc composite blown films
- Figure 6.17 XRD results (a) intensity versus 2θ curves (b) % crystallinity of PLA/PCL/talc composites

LIST OF TABLES

Sr. No.

Title

Chapter 1

Table 1.1	Unit Structure of typical biodegradable aliphatic polyesters
Table 1.2	Thermal properties of amorphous, crystalline and stereocomplex PLA
Table 1.3	Comparison of mechanical properties of PLA, PS and PET films
Table 1.4	Properties of various grade of PLA
Table 1.5	Potential applications of PLA
Table 1.6	Commercial producers of PLA and its trade names
Table 1.7	PLA blends with nonbiodegradable polymers
Table 1.8	PLA blends with various biodegradable polymers

Chapter 2

Table 2.1	Characteristics of PLA (NatureWorks® 4032D)
Table 2.2	Characteristics of PCL (CAPA® 6800)
Table 2.3	Characteristics of talc
Table 2.4	Specification of the twin screw extruder
Table 2.5	Temperature profile in the extruder during processing
Table 2.6	Formulations of (a) PLA/talc composites (b) PLA/PCL blends (c) PLA/PCL/talc composites
Table 2.7	Characteristics of soil
Table 2.8	Monthly weather condition as per RDWR (Delhi), Indian Meteorological Department, Government of India

Chapter 3

Table 3.1	Spherulite radius and nucleation density of PLA/talc composites
Table 3.2	Spherulite radius and growth rate of PLA/PCL blends

Chapter 4

Table 4.1	Avrami exponent (n) for different nucleation and growth mechanism
Table 4.2	DSC data of PLA/talc composites
Table 4.3	Isothermal crystallization kinetics data of PLA/talc composites
Table 4.4	Crystallization data for neat PLA at different heating rates
Table 4.5	Nonisothermal crystallization kinetics data of PLA/talc composites
Table 4.6	Thermogravimetric analysis (TGA) data of PLA/talc composites
Table 4.7	DSC data of PLA/PCL blends
Table 4.8	Thermogravimetric analysis (TGA) data of PLA/PCL blends
Table 4.9	DSC data of PLA/PCL/talc composites
Table 4.10	Thermogravimetric analysis (TGA) data of PLA/PCL/talc composites

Chapter 5

Table 5.1	Rheological parameters of PLA/talc composites
Table 5.2	Blown film characteristics at different nip-roll speed of PLA and PLA/talc composite
Table 5.3	Blown film characteristics of PLA/talc composite films
Table 5.4	Rheological parameters of PLA/PCL blends
Table 5.5	Blown film characteristics of PLA/PCL blend films
Table 5.6	Rheological parameters of PLA/PCL/talc composites
Table 5.7	Blown film characteristics of PLA/PCL/talc composite films

Chapter 6

Table 6.1	Dynamic mechanical analysis (DMA) of PLA/talc composites
Table 6.2	Water vapor barrier properties of PLA/talc composite blown films

Abbreviations

M_n = number average molecular weight

M_w = weight average molecular weight

wt% = weight percentage

W_f = weight fraction

D_n = number average diameter of domains (μm)

G = spherulite growth rate ($\mu\text{m}/\text{min}$)

$R_{s\text{-avg}}$ = average spherulite radius (μm)

N = nucleation density (μm^{-3})

T_g = glass transition temperature ($^{\circ}\text{C}$)

T_{m1} = temperature at first melting peak ($^{\circ}\text{C}$)

T_{m2} = temperature at second melting peak ($^{\circ}\text{C}$)

T_m = melting temperature ($^{\circ}\text{C}$)

T_p = crystallization peak temperature from cooling exotherm ($^{\circ}\text{C}$)

$T_{\text{cc-onset}}$ = onset temperature of cold crystallization ($^{\circ}\text{C}$)

T_{ccp} = cold crystallization peak temperature ($^{\circ}\text{C}$)

T_c = Temperature for isothermal crystallization conditions ($^{\circ}\text{C}$)

ΔH_m = melting enthalpy (J/g)

ΔH_{m-100} = melting enthalpy for 100% crystalline polymer (J/g)

ΔH_c = enthalpy of crystallization (J/g)

ΔH_{cc} = enthalpy of cold crystallization (J/g)

X_m = degree of crystallinity for melting endotherm (%)

X_c = degree of crystallinity from cooling exotherm (%)

X_{cc} = degree of crystallinity from cold crystallization peak (%)

ΔW_{cc} = width of cold crystallization peak at half height ($^{\circ}\text{C}$)

ΔW_m = width of melting peak at half height ($^{\circ}\text{C}$)

α = relative crystallinity (%)

K_a = crystallization rate constant from Avrami equation (min^{-1})

n = Avrami exponent

$t_{1/2}$ = crystallization half time (min)

Δt = time where crystallization reaches maximum (min)

ΔE_a = activation energy barrier (KJ/mol)

t_p = crystallization time at peak (min)

t_{max} = maximum time for crystallization (min)

ϕ = heating rate ($^{\circ}$ C/min)

R^g = gas constant (J/mol/K)

T_{onset} = temperature at 5 % weight loss ($^{\circ}$ C)

T_{max} = temperature at 50 % weight loss ($^{\circ}$ C)

T_{end} = temperature at 90 % weight loss ($^{\circ}$ C)

$DTG-T_{p-PLA}$ = degradation peak of PLA in DTG curve ($^{\circ}$ C)

$DTG-T_{p-PCL}$ = degradation peak of PCL in DTG curve ($^{\circ}$ C)

G' = Storage modulus (MPa)

G'' = loss modulus (MPa)

$\tan\delta$ = damping behavior (G''/G')

η^* = complex viscosity ($\eta' - i\eta''$) (Pa.s)

n = power law index